Iterative methods for neutron transport eigenvalue problems *

Fynn Scheben † Ivan G. Graham ‡

Abstract

We discuss iterative methods for computing criticality in nuclear reactors. In general this requires the solution of a generalised eigenvalue problem for an unsymmetric integro-differential operator in 6 independent variables, modelling transport, scattering and fission, where the dependent variable is the neutron angular flux. In engineering practice this problem is often solved iteratively, using some variant of the inverse power method. Because of the high dimension, matrix representations for the operators are often not available and the inner solves needed for the eigenvalue iteration are implemented by matrix-free inner iterations. This leads to technically complicated inexact iterative methods, for which there appears to be no published rigorous convergence theory. For the monoenergetic homogeneous model case with isotropic scattering and vacuum boundary conditions, we show that the general nonsymmetric eigenproblem for the angular flux is equivalent to a certain related eigenproblem for the scalar flux, involving a symmetric positive definite weakly singular integral operator (in space only). This correspondence to a symmetric problem (in a space of reduced dimension) permits us to give a convergence theory for inexact inverse iteration and related methods. In particular this theory provides rather precise criteria on how accurate the inner solves need to be in order for the whole iterative method to converge. The theory is illustrated with numerical computations on a homogeneous benchmark problem from the Los Alamos test set and also on an inhomogeneous bienergetic control rod problem, using GMRES as the inner solver.

1 Reactor criticality problems

Climate change is a challenging problem of great contemporary interest. It is still open to debate if nuclear power is a solution to this problem or not, but certainly ensuring the safety and optimal performance of existing nuclear reactors is an important task of great environmental significance. When operating a nuclear reactor, the engineer seeks to achieve a sustainable chain reaction where the neutrons produced balance the neutrons that are either absorbed or leave the system through the outer boundary. The chain reaction depends on the material composition and geometry of the reactor and can be controlled by inserting or removing control rods.

Mathematically the problem of modelling this balance may be written as

$$\mathcal{T}\Psi \;-\; \mathcal{S}\Psi \;=\; \lambda\,\mathcal{F}\Psi\;, \tag{1}$$

where $\Psi(\mathbf{r}, E, \mathbf{\Omega})$ is the flux of neutrons per unit volume with energy $E \in \mathbb{R}^+$ at position $\mathbf{r} \in \mathbb{R}^3$ in direction $\mathbf{\Omega} \in \mathbb{S}^2$ (the unit sphere in $\mathbb{R}^3$) and the operators $\mathcal{T}$, $\mathcal{S}$ and $\mathcal{F}$ describing, respectively, transport, scattering and fission in the reactor are given by

$$\begin{aligned}
\mathcal{T}\Psi &= \mathbf{\Omega}.\nabla\Psi(\mathbf{r}, E, \mathbf{\Omega}) \,+\, \sigma(\mathbf{r}, E)\Psi(\mathbf{r}, E, \mathbf{\Omega}) \\
\mathcal{S}\Psi &= \frac{1}{4\pi}\int_{\mathbb{R}^+}\int_{\mathbb{S}^2} \sigma_s(\mathbf{r}, E', E, \mathbf{\Omega}', \mathbf{\Omega})\Psi(\mathbf{r}, E', \mathbf{\Omega}')\,\mathrm{d}\mathbf{\Omega}'\,\mathrm{d}E' \\
\mathcal{F}\Psi &= \frac{\chi(E)}{4\pi}\int_{\mathbb{R}^+} \nu(\mathbf{r}, E')\sigma_f(\mathbf{r}, E')\int_{\mathbb{S}^2}\Psi(\mathbf{r}, E', \mathbf{\Omega}')\,\mathrm{d}\mathbf{\Omega}'\,\mathrm{d}E'
\end{aligned}$$

*We thank Melina Freitag and Alastair Spence (University of Bath), as well as Paul Smith (Serco Technical and Assurance Services) for useful discussions.

†Department of Mathematical Sciences, University of Bath, Bath BA2 7AY, UK. F.Scheben@bath.ac.uk

‡Department of Mathematical Sciences, University of Bath, Bath BA2 7AY, UK. I.G.Graham@bath.ac.uk

(see e.g. [10, (1-16),(1-104)]). Here σ_s and σ_f are the *scattering and fission cross-sections*, ν is the *neutron yield* and χ is the *fission neutron distribution*. The *total cross-section* σ is defined by

$$\sigma(\mathbf{r}, E) \;=\; \sigma_c(\mathbf{r}, E) \;+\; \frac{1}{4\pi} \int_{\mathbb{R}^+} \int_{\mathbb{S}^2} \sigma_s(\mathbf{r}, E', E, \mathbf{\Omega}', \mathbf{\Omega}) \, \mathrm{d}\mathbf{\Omega}' \, \mathrm{d}E' \;+\; \sigma_f(\mathbf{r}, E) \; .$$

Equation (1) is to be solved for $\mathbf{r}$ in some sufficiently smooth bounded domain $V \subset \mathbb{R}^3$, subject to suitable boundary conditions (see below for an example). The eigenvalue λ with smallest modulus has direct physical meaning: Using Krein-Rutman arguments, under quite general assumptions, this can be shown to be real, positive and simple [12]. The value of λ describes the balance between transport and scattering on one hand and fission on the other. The reactor is called *subcritical* if $\lambda > 1$, *supercritical* if $\lambda < 1$ and *critical* if $\lambda = 1$. Designing a reactor so that λ is close to 1 is a key inverse problem in nuclear engineering. To do this we need efficient methods to compute λ for any given reactor (the forward problem) and that is the focus of this paper.

We note that there is a large amount of background literature on neutron transport theory and nuclear engineering (for example [3, 10] and [16]). There has also been widespread interest from numerical analysts (e.g. [2, 8, 11, 13]), but this activity is related mainly to the solution of source problems where a unique solution Ψ to (1) is to be found subject to given λ and with the addition of a forcing term on the right-hand side. Some discretisation error estimates for computed eigenvalues are given for example in [2] and [13] and a brief discussion of the inverse power method in the context of neutron transport is in [1], but we do not know of any literature giving rigorous convergence results for iterative methods for the neutron criticality problem.

Model problems. Now let us consider the homogeneous model problem of isotropic scattering in the monoenergetic case subject to vacuum boundary conditions. Then $\chi = 1$ and all the cross-sections are constant with $\sigma = \sigma_c + \sigma_s + \sigma_f$. In this reactor the neutrons travel with the same constant speed and no neutrons enter the reactor from the outside.

3D model. In the most general 3D case (1) then takes the form

$$\mathbf{\Omega}.\nabla\Psi(\mathbf{r}, \mathbf{\Omega}) \;+\; \sigma\Psi(\mathbf{r}, \mathbf{\Omega}) \;-\; \frac{\sigma_s}{4\pi} \int_{\mathbb{S}^2} \Psi(\mathbf{r}, \mathbf{\Omega}') \, \mathrm{d}\mathbf{\Omega}' \;=\; \lambda \, \frac{\nu\sigma_f}{4\pi} \int_{\mathbb{S}^2} \Psi(\mathbf{r}, \mathbf{\Omega}') \, \mathrm{d}\mathbf{\Omega}' \tag{2}$$

and this is to be solved for all $(\mathbf{r}, \mathbf{\Omega}) \in V \times \mathbb{S}^2$, subject to

$$\Psi(\mathbf{r}, \mathbf{\Omega}) = 0 \quad \text{when} \quad \mathbf{n}(\mathbf{r}).\mathbf{\Omega} \;<\; 0 \; , \quad \mathbf{r} \in \partial V \; , \tag{3}$$

where $\mathbf{n}(\mathbf{r})$ denotes the outward unit normal at $\mathbf{r} \in \partial V$, the boundary of V.

Two subcases of this have received some attention in the literature. To describe them, let $(\theta, \varphi) \in [0, \pi] \times [0, 2\pi]$ denote the usual spherical polar coordinates on $\mathbb{S}^2$.

2D model. Here it is assumed that $\Psi(\mathbf{r}, \mathbf{\Omega}) = \Psi(\tilde{\mathbf{r}}, \widetilde{\mathbf{\Omega}})$ where $\widetilde{\mathbf{r}} \in \widetilde{V} \subset \mathbb{R}^2$ and $\widetilde{\mathbf{\Omega}} = (\cos\theta, \sin\theta)$ lies on the unit circle $\mathbb{S}^1$. The resulting model problem

$$\widetilde{\mathbf{\Omega}}.\widetilde{\nabla}\Psi(\widetilde{\mathbf{r}}, \widetilde{\mathbf{\Omega}}) \;+\; \sigma\Psi(\widetilde{\mathbf{r}}, \widetilde{\mathbf{\Omega}}) \;-\; \frac{\sigma_s}{2\pi} \int_{\mathbb{S}^1} \Psi(\widetilde{\mathbf{r}}, \widetilde{\mathbf{\Omega}}') \, \mathrm{d}\widetilde{\mathbf{\Omega}}' \;=\; \lambda \, \frac{\nu\sigma_f}{2\pi} \int_{\mathbb{S}^1} \Psi(\widetilde{\mathbf{r}}, \widetilde{\mathbf{\Omega}}') \, \mathrm{d}\widetilde{\mathbf{\Omega}}'$$

is to be solved on $\widetilde{V} \times \mathbb{S}^1$ (where $\widetilde{\nabla}$ denotes the 2D gradient), subject to

$$\Psi(\widetilde{\mathbf{r}}, \widetilde{\mathbf{\Omega}}) = 0 \quad \text{when} \quad \tilde{\mathbf{n}}(\widetilde{\mathbf{r}}).\widetilde{\mathbf{\Omega}} \;<\; 0 \; , \quad \widetilde{\mathbf{r}} \in \partial\widetilde{V} \; ,$$

where $\tilde{\mathbf{n}}(\tilde{\mathbf{r}})$ again denotes the outward unit normal at $\tilde{\mathbf{r}} \in \partial\widetilde{V}$ (see e.g. [2] and the references therein).

1D model. Here it is assumed that $\Psi(\mathbf{r}, \mathbf{\Omega}) = \Psi(z, \mu)$ where $z \in [0, 1]$ and $\mu = \cos\theta \in [-1, 1]$, and (2), (3) reduce to

$$\mu \frac{\partial}{\partial z}\Psi(z, \mu) \;+\; \sigma\Psi(z, \mu) \;-\; \frac{\sigma_s}{2} \int_{-1}^{1} \Psi(z, \mu') \, \mathrm{d}\mu' \;=\; \lambda \, \frac{\nu\sigma_f}{2} \int_{-1}^{1} \Psi(z, \mu') \, \mathrm{d}\mu' \tag{4}$$

to be solved on $[0,1]\times[-1,1]$, subject to

$$\Psi(0,\mu)=0 \quad \text{when} \quad \mu>0 \quad \text{and} \quad \Psi(1,\mu)=0 \quad \text{when} \quad \mu<0\ . \tag{5}$$

This ("1D slab geometry") model has received a lot of attention in the literature (e.g. in [11, 13]).

In section 2 we establish the relation of all three model problems to a symmetric positive definite integral operator eigenvalue problem. We then discuss iterative methods for the computation of the eigenvalue (section 3) and study their convergence. In section 4 we give numerical results which illustrate the theory.

2 Relation to a symmetric problem

The key to the reduction to a symmetric problem is to introduce the scalar flux

$$\phi(\mathbf{r}) \;=\; \mathcal{P}\Psi \;:=\; \frac{1}{4\pi}\int_{\mathbb{S}^2}\Psi(\mathbf{r},\mathbf{\Omega}')\,\mathrm{d}\mathbf{\Omega}'\ .$$

We show that ϕ satisfies a certain integral equation with a symmetric operator. The argument is well known - see e.g. [10], or [2, 13] for 2D and 1D analogues.

Lemma 2.1. *Suppose* Ψ *satisfies* $\mathcal{T}\Psi(\mathbf{r},\mathbf{\Omega})=\mathbf{\Omega}.\nabla\Psi(\mathbf{r},\mathbf{\Omega})+\sigma\Psi(\mathbf{r},\mathbf{\Omega})=g(\mathbf{r},\mathbf{\Omega})$ *and* (3). *Then*

$$\left(\mathcal{T}^{-1}g\right)(\mathbf{r},\mathbf{\Omega}) \;=\; \Psi(\mathbf{r},\mathbf{\Omega}) \;=\; \int_0^{d(\mathbf{r},\mathbf{\Omega})}\exp(-\sigma s)g(\mathbf{r}-s\mathbf{\Omega},\mathbf{\Omega})\,\mathrm{d}s\ , \tag{6}$$

where $d(\mathbf{r},\mathbf{\Omega}):=\inf\{s>0:\mathbf{r}-s\mathbf{\Omega}\notin V\}$. *Moreover, if* (λ,Ψ) *is an eigenpair for* (2), *then*

$$\phi(\mathbf{r})-\sigma_s\mathcal{K}_\sigma\phi(\mathbf{r}) \;=\; \lambda\ \nu\sigma_f\mathcal{K}_\sigma\phi(\mathbf{r})\ , \quad \mathbf{r}\in V\ ,$$

$$\text{where}\quad (\mathcal{K}_\sigma g)(\mathbf{r}):=\int_V k_\sigma(\mathbf{r}-\mathbf{r}')g(\mathbf{r}')\,\mathrm{d}\mathbf{r}'\ , \quad \text{with}\quad k_\sigma(\mathbf{x}):=\frac{1}{4\pi}\,\frac{\exp(-\sigma\|\mathbf{x}\|_2)}{\|\mathbf{x}\|_2^2}\ , \quad \mathbf{x}\in\mathbb{R}^3\ . \tag{7}$$

Proof. Provided $\mathbf{r}-s\mathbf{\Omega}\in V$, we have $-\frac{\mathrm{d}}{\mathrm{d}s}\left[\Psi(\mathbf{r}-s\mathbf{\Omega},\mathbf{\Omega})\exp(-\sigma s)\right] \;=\; g(\mathbf{r}-s\mathbf{\Omega},\mathbf{\Omega})\exp(-\sigma s)$. Integrating from $s=0$ to $s=d(\mathbf{r},\mathbf{\Omega})$, we obtain (6), and applying $\mathcal{P}$ yields

$$\phi(\mathbf{r}) \;=\; \int_{\mathbb{S}^2}\int_0^{d(\mathbf{r},\mathbf{\Omega})}\frac{\exp(-\sigma s)}{4\pi s^2}\,g(\mathbf{r}-s\mathbf{\Omega},\mathbf{\Omega})\,s^2\,\mathrm{d}s\,\mathrm{d}\mathbf{\Omega}\ .$$

Now, if $g(\mathbf{r},\mathbf{\Omega})=g(\mathbf{r})$, and using spherical coordinates centred at $\mathbf{r}$ with $\mathbf{r}'=\mathbf{r}-s\mathbf{\Omega}$, we obtain $\phi=\mathcal{K}_\sigma g$. Applying this to equation (2) by choosing $g=(\sigma_s+\lambda\ \nu\sigma_f)\,\phi$, and using the linearity of $\mathcal{K}_\sigma$, we obtain the result. □

Remark 2.2. *An analogous argument can be applied to the 2D and 1D model problems.*
For the 2D problem the result is

$$\phi(\widetilde{\mathbf{r}})-\sigma_s\mathcal{K}_\sigma\phi(\widetilde{\mathbf{r}}) \;=\; \lambda\ \nu\sigma_f\mathcal{K}_\sigma\phi(\widetilde{\mathbf{r}})\ , \quad \text{where}\quad \phi(\widetilde{\mathbf{r}}):=\frac{1}{2\pi}\int_{\mathbb{S}^2}\Psi(\widetilde{\mathbf{r}},\widetilde{\mathbf{\Omega}}')\,\mathrm{d}\widetilde{\mathbf{\Omega}}'\ ,$$

$$\text{and}\qquad (\mathcal{K}_\sigma g)(\widetilde{\mathbf{r}}):=\int_V k_\sigma(\widetilde{\mathbf{r}}-\widetilde{\mathbf{r}}')g(\widetilde{\mathbf{r}}')\,\mathrm{d}\widetilde{\mathbf{r}}'\ , \quad \text{with}\quad k_\sigma(\mathbf{x}):=\frac{1}{2\pi}\,\frac{\exp(-\sigma\|\mathbf{x}\|_2)}{\|\mathbf{x}\|_2}\ , \quad \mathbf{x}\in\mathbb{R}^2\ .$$

For the 1D problem the result is

$$\phi(z)-\sigma_s\mathcal{K}_\sigma\phi(z) \;=\; \lambda\ \nu\sigma_f\mathcal{K}_\sigma\phi(z)\ , \quad \text{where}\quad \phi(z):=\frac{1}{2}\int_{-1}^{1}\Psi(z,\mu')\,\mathrm{d}\mu'\ ,$$

$$\text{and}\qquad (\mathcal{K}_\sigma g)(z):=\int_0^1 k_\sigma(z-z')g(z')\,\mathrm{d}z'\ , \quad \text{with}\quad k_\sigma(x):=\frac{1}{2}\int_0^1\exp\left(\frac{-\sigma|x|}{\mu}\right)\frac{\mathrm{d}\mu}{\mu}\ .$$

In all instances the operator $\mathcal{K}_\sigma$ is clearly symmetric and by [9] it is compact on $L^2(V)$. In fact, as we show in the next lemma, all the eigenvalues of $\mathcal{K}_\sigma$ in (7) are positive which ensures (e.g. [14]) that $\mathcal{K}_\sigma$ is positive definite.

Lemma 2.3. *All the eigenvalues of the operator $\mathcal{K}_\sigma$ are positive. Moreover, $\|\mathcal{K}_\sigma\|_{\mathscr{L}(L^2(V))} \leq \sigma^{-1}$.*

Proof. Suppose $\mathcal{K}_\sigma f = \omega f$ for some eigenvalue ω which must be real. Let $\Psi(\mathbf{r}, \mathbf{\Omega})$ be the solution of $\mathbf{\Omega}.\nabla\Psi + \sigma\Psi = f$ on $V \times \mathbb{S}^2$, subject to vacuum boundary conditions (3). Then, by Lemma 2.1, the corresponding scalar flux satisfies $\phi = \mathcal{K}_\sigma f = \omega f$, and we have

$$\begin{aligned} \omega f^2(\mathbf{r}) \;=\; \phi(\mathbf{r})f(\mathbf{r}) \;&=\; \frac{1}{4\pi}\int_{\mathbb{S}^2} \Psi(\mathbf{r},\mathbf{\Omega}) f(\mathbf{r})\,\mathrm{d}\mathbf{\Omega} \\ &=\; \frac{1}{4\pi}\int_{\mathbb{S}^2} \mathbf{\Omega}.\left[\Psi(\mathbf{r},\mathbf{\Omega})\nabla\Psi(\mathbf{r},\mathbf{\Omega})\right]\mathrm{d}\mathbf{\Omega} \;+\; \frac{\sigma}{4\pi}\int_{\mathbb{S}^2}\Psi^2(\mathbf{r},\mathbf{\Omega})\,\mathrm{d}\mathbf{\Omega}\,. \end{aligned}$$

Integrating over V and applying the divergence theorem, the first term on the right hand side becomes

$$\begin{aligned} \frac{1}{4\pi}\int_{\mathbb{S}^2}\mathbf{\Omega}.\left[\int_V \Psi(\mathbf{r},\mathbf{\Omega})\nabla\Psi(\mathbf{r},\mathbf{\Omega})\,\mathrm{d}\mathbf{r}\right]\mathrm{d}\mathbf{\Omega} \;&=\; \frac{1}{8\pi}\int_{\mathbb{S}^2}\mathbf{\Omega}.\left[\int_V \nabla\left[\Psi^2(\mathbf{r},\mathbf{\Omega})\right]\,\mathrm{d}\mathbf{r}\right]\mathrm{d}\mathbf{\Omega} \\ &=\; \frac{1}{8\pi}\int_{\mathbb{S}^2}\int_{\partial V}\Psi^2(\mathbf{r},\mathbf{\Omega})\,\left[\mathbf{\Omega}.\mathbf{n}(\mathbf{r})\right]\,\mathrm{d}\mathbf{r}\,\mathrm{d}\mathbf{\Omega} \;\geq\; 0\,, \end{aligned}$$

where we used (3) for the final estimate. Hence $\omega\int_V f^2(\mathbf{r})\,\mathrm{d}\mathbf{r} \geq \frac{\sigma}{4\pi}\int_V\int_{\mathbb{S}^2}\Psi^2(\mathbf{r},\mathbf{\Omega})\,\mathrm{d}\mathbf{\Omega}\,\mathrm{d}\mathbf{r}$, and finally, as $f \neq 0$, the integrals on both sides are positive and it follows that $\omega > 0$.

To prove the bound on the norm, note that $\mathcal{K}_\sigma\phi = k_\sigma * \phi^e$, where ϕ^e is the trivial extension of ϕ to all of $\mathbb{R}^3$ by choosing ϕ^e to be zero outside of V, and $*$ denotes convolution on $\mathbb{R}^3$. Then, by Young's inequality and a simple computation, $\|\mathcal{K}_\sigma\|_{\mathscr{L}(L^2(V))} \leq \|k_\sigma\|_{L^1(\mathbb{R}^3)} = \sigma^{-1}$. There are analogous arguments for the 2D and 1D problems but we omit them here. □

Now we define for functions $v(\mathbf{x}, \mathbf{\Omega})$ the scalar quantity

$$\|v\|_* \;=\; \|\mathcal{P}\mathcal{T}^{-1}v\|_{L^2(V)}\,.$$

If $v(\mathbf{x}, \mathbf{\Omega}) = v(\mathbf{x})$, for all $(\mathbf{x}, \mathbf{\Omega}) \in V \times \mathbb{S}^2$, we have $\|v\|_* = \|\mathcal{K}_\sigma v\|_{L^2(V)}$, so that $\|\cdot\|_*$ acts as a norm on the subspace of all functions in $L^2(V \times \mathbb{S}^2)$ which are constant with respect to their second argument.

3 Iterative methods for reactor criticality

Since $\mathcal{K}_\sigma$ is symmetric and compact on $L^2(V)$, it has an infinite sequence of orthonormal eigenpairs $(\omega_j, e_j)_{j=1}^\infty$ where $\mathcal{K}_\sigma e_j = \omega_j e_j$, and where ω_j are positive, monotone non-increasing and converge to 0 as $j \to \infty$. Thus, the eigenvalues λ in Lemma 2.1 are

$$\lambda_j \;:=\; \frac{1 - \sigma_s\omega_j}{\nu\sigma_f\omega_j}\,. \tag{8}$$

Moreover, from Lemma 2.3, and the fact that $\sigma = \sigma_c + \sigma_s + \sigma_f$ (and all cross-sections are positive), we have $\sigma_s\omega_j \leq \sigma_s\sigma^{-1} < 1$. So the λ_j are positive, non-decreasing and approach ∞ as $j \to \infty$. In fact, a Krein-Rutman argument (see [12]) shows that λ_1 (the eigenvalue of physical interest) is simple. Now, for any $\phi \in L^2(V)$, we can write $\phi = \sum_{j=1}^\infty \xi_j(\phi)e_j$, where $\xi_j(\phi) = (\phi, e_j)_{L^2(V)}$, and we have

$$\|\phi\|^2_{L^2(V)} \;=\; \sum_{j=1}^\infty |\xi_j(\phi)|^2 \;=\; c(\phi)^2 + s(\phi)^2 \tag{9}$$

(Parseval's equality), where $c(\phi) := |\xi_1(\phi)|$ and $s(\phi)^2 := \sum_{j=2}^\infty |\xi_j(\phi)|^2$ and $t(\phi) := s(\phi)/c(\phi)$.

The following algorithm is a simple version of inexact inverse iteration stated as an infinite loop.

Algorithm 1 Inexact inverse iteration with shift

Require: Starting guess $\Psi^{(0)}$.
  for i=0,1,2,... **do**
    Choose a shift $\alpha^{(i)}$ and an inner tolerance $\tau^{(i)} \geq 0$.
    Compute $\tilde{\Psi}^{(i+1)}$ so that $\|(\mathcal{T}-\mathcal{S}-\alpha^{(i)}\mathcal{F})\tilde{\Psi}^{(i+1)} - \mathcal{F}\Psi^{(i)}\|_* \leq \tau^{(i)}$. (†)
    Normalise $\Psi^{(i+1)} = \tilde{\Psi}^{(i+1)}/\|\mathcal{P}\tilde{\Psi}^{(i+1)}\|_{L^2(V)}$.
  end for

We typically stop this algorithm if the eigenvalue residual $\mathbf{res}^{(i)} := (\mathcal{T}-\mathcal{S}-\rho^{(i)}\mathcal{F})\Psi^{(i)}$ is sufficiently small in some norm, where $\rho^{(i)}$ is a suitable eigenvalue approximation (e.g. a Rayleigh quotient) derived from $\Psi^{(i)}$ when $\Psi^{(i)}$ is rich in a certain eigendirection. We discuss a particular choice of $\rho^{(i)}$ below. Now observe that if $\Psi^{(i)}$ is computed by Algorithm 1, and if we introduce the corresponding scalar fluxes $\phi^{(i)} = \mathcal{P}\Psi^{(i)}$ and $\tilde{\phi}^{(i)} = \mathcal{P}\tilde{\Psi}^{(i)}$, then

$$\|(I-(\sigma_s+\alpha^{(i)}\nu\sigma_f)\mathcal{K}_\sigma)\tilde{\phi}^{(i+1)} - \nu\sigma_f\mathcal{K}_\sigma\phi^{(i)}\|_{L^2(V)} \leq \tau^{(i)} \quad \text{and} \quad \phi^{(i+1)} = \tilde{\phi}^{(i+1)}/\|\tilde{\phi}^{(i+1)}\|_{L^2(V)}\,. \tag{10}$$

When $\Psi^{(i)}$ is close to an eigenvector corresponding to the minimal eigenvalue of (1), then $\phi^{(i)}$ is predominantly in the direction e_1 and $c(\phi^{(i)})$ will approach 1, while $s(\phi^{(i)})$ and $t(\phi^{(i)})$ will tend to 0. The following theorem gives a mechanism for bounding $t(\phi^{(i+1)})$ and hence assessing the convergence of Algorithm 1. For convenience we will discuss an abstract version of (10) where the superscripts are suppressed.

Theorem 3.1. *Suppose* $s(\phi) \neq 0$ *and*

$$\|(I-(\sigma_s+\alpha\,\nu\sigma_f)\mathcal{K}_\sigma)\tilde{\phi} - \nu\sigma_f\mathcal{K}_\sigma\phi\|_{L^2(V)} < \tau\,, \quad \textit{and set} \quad \phi' = \tilde{\phi}/\|\tilde{\phi}\|_{L^2(V)}\,. \tag{11}$$

Then, if $\tau < \nu\sigma_f\omega_1 c(\phi)$, *we have*

$$t(\phi') \leq \frac{\omega_1}{\omega_2}\left(\frac{\nu\sigma_f\omega_2 s(\phi)+\tau}{\nu\sigma_f\omega_1 c(\phi)-\tau}\right)\left|\frac{\lambda_1-\alpha}{\lambda_2-\alpha}\right|\,. \tag{12}$$

Proof. To make the notation simpler, set $\nu = 1$ in the proof. Note that if $\tilde{\phi} = 0$ in (11) and $s(\phi) \neq 0$,

$$\tau \geq \sigma_f\|\mathcal{K}_\sigma\phi\|_{L^2(V)} = \sigma_f\left\{\sum_{j=1}^{\infty}\omega_j^2|\xi_j(\phi)|^2\right\}^{1/2} > \sigma_f\omega_1 c(\phi)\,,$$

which is impossible and so the normalisation step in (11) makes sense. To obtain the bound on $t(\phi')$, let us introduce the quantity $R := (I-(\sigma_s+\alpha\sigma_f)\mathcal{K}_\sigma)\tilde{\phi} - \sigma_f\mathcal{K}_\sigma\phi$. Because the (ω_j, e_j) are eigenpairs of $\mathcal{K}_\sigma$, we have (using (11) and (8)), for all $j \geq 1$,

$$\xi_j(R) = (1-(\sigma_s+\alpha\sigma_f)\omega_j)\xi_j(\tilde{\phi}) - \sigma_f\omega_j\xi_j(\phi) = \sigma_f\omega_j\left[\|\tilde{\phi}\|_{L^2(V)}(\lambda_j-\alpha)\xi_j(\phi') - \xi_j(\phi)\right]\,. \tag{13}$$

Now using (9) and (11), we have $\tau \geq \|R\|_{L^2(V)} \geq |\xi_1(R)| \geq \sigma_f\omega_1\left[c(\phi) - \|\tilde{\phi}\|_{L^2(V)}\,|\lambda_1-\alpha|\,c(\phi')\right]$, and a rearrangement of this yields

$$\frac{c(\phi)}{c(\phi')} \leq \left(\frac{\sigma_f\omega_1 c(\phi)}{\sigma_f\omega_1 c(\phi)-\tau}\right)|\lambda_1-\alpha|\,\|\tilde{\phi}\|_{L^2(V)}\,. \tag{14}$$

On the other hand, rearranging (13) gives

$$\xi_j(\phi')\|\tilde{\phi}\|_{L^2(V)} = \left(\frac{1}{\lambda_j-\alpha}\right)\left[\frac{\xi_j(R)}{\sigma_f\omega_j} + \xi_j(\phi)\right]\,. \tag{15}$$

Now recall that λ_j increases and that (via (8)) $\sigma_f(\lambda_j - \alpha)\omega_j = 1 - (\sigma_s + \sigma_f\alpha)\omega_j$ which increases as well. Hence, summing (15) over $j = 2, \ldots, \infty$, and recalling (11), we obtain

$$s(\phi')\|\tilde{\phi}\|_{L^2(V)} \;\leq\; \frac{1}{|\lambda_2 - \alpha|}\left(\frac{\tau}{\sigma_f\omega_2} \;+\; s(\phi)\right) . \tag{16}$$

Finally, by rearranging the product of (14) and (16), we obtain the result. □

Given $\Psi^{(i)}$, an approximation to the corresponding eigenvalue is obtained by the particular Rayleigh quotient

$$\rho^{(i)} \;:=\; \frac{(\mathcal{P}\Psi^{(i)}, \mathcal{P}\mathcal{T}^{-1}(\mathcal{T} - \mathcal{S})\Psi^{(i)})_{L^2(V)}}{(\mathcal{P}\Psi^{(i)}, \mathcal{P}\mathcal{T}^{-1}\mathcal{F}\Psi^{(i)})_{L^2(V)}} \;=\; \frac{(\phi^{(i)}, (I - \sigma_s\mathcal{K}_\sigma)\phi^{(i)})_{L^2(V)}}{(\phi^{(i)}, \nu\sigma_f\mathcal{K}_\sigma\phi^{(i)})_{L^2(V)}} . \tag{17}$$

For this choice, and by writing $\phi^{(i)} = c(\phi^{(i)})e_1 + s(\phi^{(i)})u^{(i)}$, where $\|u^{(i)}\|_{L^2(V)} = 1$, $(u^{(i)}, e_1)_{L^2(V)} = 0$, and using (8), we see that

$$\rho^{(i)} \;=\; \frac{(1 - \sigma_s\omega_1)\, c(\phi^{(i)})^2 \;+\; O(s(\phi^{(i)})^2)}{\nu\sigma_f\omega_1\, c(\phi^{(i)})^2 \;+\; O(s(\phi^{(i)})^2)} \;=\; \lambda_1 \;+\; O(s(\phi^{(i)})^2) .$$

If we now apply Algorithm 1 with $\alpha^{(i)} = \rho^{(i)}$ (Rayleigh Quotient Iteration), then Theorem 3.1 gives

$$t(\phi^{(i+1)}) \;\leq\; \frac{\omega_1}{\omega_2}\left(\frac{\sigma_f\omega_2 s(\phi^{(i)}) + \tau^{(i)}}{\sigma_f\omega_1 c(\phi^{(i)}) - \tau^{(i)}}\right)\left|\frac{C}{\lambda_2 - \lambda_1}\right|\; t(\phi^{(i)})^2 , \quad C \text{ constant} ,$$

indicating that Algorithm 1 converges quadratically. We even obtain cubic convergence if the tolerances decrease with rate

$$\tau^{(i)} \;\leq\; C' s(\phi^{(i)}) , \quad C' \text{ constant} . \tag{18}$$

On the other hand, for a fixed shift $\alpha^{(i)} = \alpha_0$, and tolerances satisfying (18), using (12) we get

$$t(\phi^{(i+1)}) \;\leq\; \frac{\omega_1}{\omega_2}\left(\frac{\sigma_f\omega_2 \;+\; C'}{\sigma_f\omega_1 c(\phi^{(i)}) - \tau^{(i)}}\right)\left|\frac{\lambda_1 - \alpha_0}{\lambda_2 - \alpha_0}\right|\; t(\phi^{(i)}) .$$

Hence, provided the shift α_0 is close enough to λ_1, we obtain linear convergence. Note that this analysis gives no guarantee that Algorithm 1 converges when we use a fixed shift and constant tolerances. In the next section we investigate this question numerically.

This type of analysis will also extend to other iterative methods such as Jacobi-Davidson (e.g. as is done in a different context in [5, 6]). The analysis here is given only for the continuous problem (1), but it provides a guide how iterations will behave in discrete cases as we see in the next section, where we investigate two 1D model problems of different complexity.

4 Numerical results

Los Alamos benchmark test set problem. This model problem is taken from a collection of benchmark tests produced at Los Alamos National Laboratory [15]. The problem number 2 there corresponds to the 1D problem (4), (5). The principal eigenvalue is equal to unity to at least five decimal places.

For our discretisation we choose a discrete ordinates approach with even order Gauss quadrature points for the angular approximation and a Crank Nicolson scheme for the spatial discretisation. Further details, as well as bounds for the discretisation error, can be found in [13]. We use for our numerical tests 144 equally sized spatial points and 128 angular Gauss points leading to a non-symmetric generalised matrix eigenvalue problem of dimension 16384×16384. The eigenvalue nearest zero of the discrete problem is $\lambda_1 \approx 1.00003$. Our stopping criterion for the outer iteration is $\|\widetilde{\mathbf{res}}\|_2 < 10^{-14}$ where $\widetilde{\mathbf{res}}^{(i)} := (T - S - \widetilde{\rho}^{(i)}F)\mathbf{\Psi}^{(i)}$ with T, S, F and $\mathbf{\Psi}$ being the discrete versions

of $\mathcal{T}$, $\mathcal{S}$, $\mathcal{F}$ and Ψ respectively and where $\widetilde{\rho}^{(i)} = \widetilde{\rho}(\mathbf{\Psi}^{(i)})$ and $\widetilde{\rho}(\mathbf{\Psi}) = (\mathbf{\Psi}, (T-S)\mathbf{\Psi})/(\mathbf{\Psi}, F\mathbf{\Psi})$ is the standard Rayleigh quotient with discrete inner product over all spatial and angular points. Note that here we compute this (outer) eigenvalue residual in the full, spatially and angular dependent space and not in the reduced space with our special Rayleigh quotient. Problem (†) in Algorithm 1 is solved using MATLAB's GMRES function with an incomplete LU factorisation of T as preconditioner which proves essential. As starting guess we use a uniform vector of ones unless specified otherwise.

Table 1 shows the results for the case of fixed shifts $\alpha_0 = 0.9$ and $\alpha_0 = 0.99$. We used decreasing tolerances $\tau^{(i)} \leq 0.1 \, \|P \, \widetilde{\mathbf{res}}\|_2$ for the inner solves, where P denotes the discrete version of the operator $\mathcal{P}$. The first two columns denote the iteration number and the corresponding eigenvalue error $\Delta^{(i)} := |\lambda_1 - \widetilde{\rho}^{(i)}|$ where λ_1 is the exact smallest eigenvalue of the discretisation. The results clearly show linear and not quadratic convergence in both cases with a faster linear rate when $\alpha = 0.99$, agreeing with our theoretical results.

	$\alpha_0 = 0.9$			$\alpha_0 = 0.99$		
i	$\Delta^{(i)}$	$\Delta^{(i)}/\Delta^{(i-1)}$	$\Delta^{(i)}/(\Delta^{(i-1)})^2$	$\Delta^{(i)}$	$\Delta^{(i)}/\Delta^{(i-1)}$	$\Delta^{(i)}/(\Delta^{(i-1)})^2$
1	2.97E-04			2.61E-05		
2	6.06E-06	2.04E-02	6.87E+01	6.36E-08	2.44E-03	9.35E+01
3	1.58E-07	2.60E-02	4.29E+03	1.71E-10	2.69E-03	4.23E+04
4	4.27E-09	2.71E-02	1.72E+05	4.80E-13	2.80E-03	1.64E+07
5	1.17E-10	2.75E-02	6.44E+06	0.00E+00	0.00E+00	0.00E+00
6	3.25E-12	2.77E-02	2.36E+08			
7	8.99E-14	2.77E-02	8.51E+09			
8	0.00E+00	0.00E+00	0.00E+00			

Table 1: Numerical results for Algorithm 1 with decreasing tolerance $\tau^{(i)} \leq 0.1 \, \|P \, \widetilde{\mathbf{res}}\|_2$.

Surprisingly, even for a fixed shift $\alpha_0 = 0.9$ and a fixed inner tolerance $\tau_0 = 0.1$, we still obtained linear convergence. This seems to be due to the fact that MATLAB's GMRES function solves the inner linear systems (†) for this model problem far more accurate than the applied tolerance of 0.1 would suggest. In practice this then results in a (slowly) decreasing inner tolerance, leading to linear convergence of the method.

Table 2 concerns the variable shift case, comparing $\alpha^{(i)} = \rho^{(i)}$, the special Rayleigh quotient from (17), and the standard Rayleigh quotient $\widetilde{\rho}^{(i)}$ above. It is difficult to judge if the predicted quadratic convergence is achieved as the method converges so fast. But the results indicate a superior convergence with the non-standard Rayleigh quotient shift compared to the standard one.

	$\alpha^{(i)} = \widetilde{\rho}^{(i)}$			$\alpha^{(i)} = \rho^{(i)}$		
i	$\Delta^{(i)}$	$\Delta^{(i)}/\Delta^{(i-1)}$	$\Delta^{(i)}/(\Delta^{(i-1)})^2$	$\Delta^{(i)}$	$\Delta^{(i)}/\Delta^{(i-1)}$	$\Delta^{(i)}/(\Delta^{(i-1)})^2$
1	2.97E-04			5.57E-05		
2	1.90E-08	6.39E-05	2.15E-01	5.11E-10	9.17E-06	1.65E-01
3	1.60E-13	8.44E-06	4.45E+02	0.00E+00	0.00E+00	0.00E+00
4	0.00E+00	0.00E+00	0.00E+00			

Table 2: Numerical results for Algorithm 1 with constant tolerance $\tau_0 = 0.1$.

Due to reaching machine precision so quickly we were not able to establish clearly the predicted cubic convergence for a Rayleigh quotient shift and decreasing tolerance. The results with the two different Rayleigh quotients and $\tau^{(i)}$, taken as in Table 1, were qualitatively similar to those in Table 2. One of the future tasks could be to redo these calculations using variable precision arithmetic.

The following numerical results are now for a more realistic problem with two different material regions and neutrons of two energy levels.

Control rod insertion model problem. This model problem describes the core of a nuclear reactor for different insertion depths of a control rod. Identical cells are usually arranged in a lattice structure or in rings surrounding a central pin. The resulting symmetry can be exploited by modelling only half of a cell and enforcing reflective boundary conditions (as indicated in the figure below). In

1D the reflective boundary conditions are (for $V = [0, 1]$ and with E denoting the energy)

$$\Psi(0, E, \mu) = \Psi(0, E, -\mu) \quad \text{when} \quad \mu > 0 \quad \text{and} \quad \Psi(1, E, \mu) = \Psi(1, E, -\mu) \quad \text{when} \quad \mu < 0 \, .$$

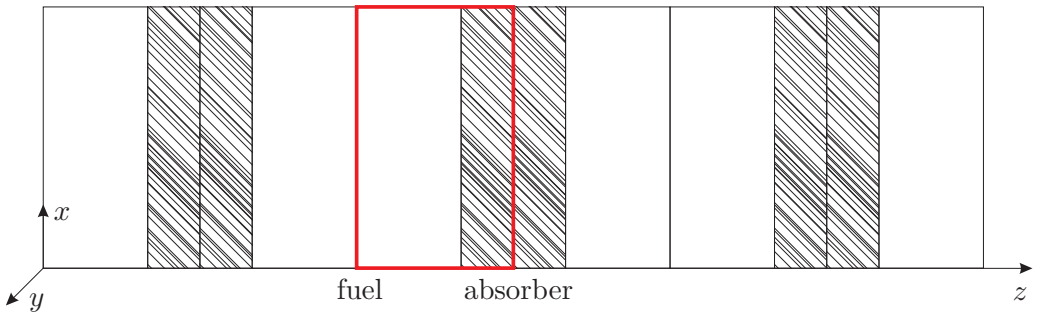

We model the problem as a slab reactor (constant flux in the x and y dimension) with two regions in the z direction, the fuel and the absorber (as shown in the figure). The latter consists of a homogenised, non-fissile mix of control rod material and remaining water if the rod is not fully inserted. Depending on the insertion depth of the control rod, the material properties in the absorber region change. Within each region we assume the material cross sections to be constant.

The energy spectrum of this model problem is constrained to neutrons of high and low energy (denoted by subscripts h and l), with angular fluxes Ψ_h and Ψ_l, which are linked by the fission and scattering operators. The latter now includes, in addition to self-scatter within the same energy group, scatter from high to low energies ($\sigma_{s,h\to l}$), and vice versa ($\sigma_{s,l\to h}$). It is assumed that all fission product neutrons are of high energy, i.e. $(\chi_h, \chi_l) = (1, 0)$. The model problem analogue to (4), but with two energy groups, is

$$\begin{aligned} &\mu \frac{\partial}{\partial z} \begin{pmatrix} \Psi_h(z,\mu) \\ \Psi_l(z,\mu) \end{pmatrix} + \begin{pmatrix} \sigma_h(z) & 0 \\ 0 & \sigma_l(z) \end{pmatrix} \begin{pmatrix} \Psi_h(z,\mu) \\ \Psi_l(z,\mu) \end{pmatrix} \\ &- \begin{pmatrix} \sigma_{s,h\to h}(z) & \sigma_{s,l\to h}(z) \\ \sigma_{s,h\to l}(z) & \sigma_{s,l\to l}(z) \end{pmatrix} \frac{1}{2} \int_{-1}^{1} \begin{pmatrix} \Psi_h(z,\mu') \\ \Psi_l(z,\mu') \end{pmatrix} \mathrm{d}\mu' \\ &= \lambda \begin{pmatrix} \nu_h(z)\sigma_{f,h}(z) & \nu_l(z)\sigma_{f,l}(z) \\ 0 & 0 \end{pmatrix} \frac{1}{2} \int_{-1}^{1} \begin{pmatrix} \Psi_h(z,\mu') \\ \Psi_l(z,\mu') \end{pmatrix} \mathrm{d}\mu' \, . \end{aligned} \tag{19}$$

The discrete ordinates method is again applied with 136 spatial points (resolving the material boundary) and 128 angles leading to a system of size 34816×34816. We investigate the convergence behaviour of Algorithm 1 with respect to three different material compositions in the absorber region: (i) The pure absorber case; (ii) a mix of 10% absorber and 90% water; and (iii) a homogeneous case, where the absorber and fuel region have the same cross sections. The principal eigenvalues in cases (i)-(iii) are $\lambda_1 \approx 1.18$, 0.92 and 0.85, respectively, and the problem details are given in Table 3.

	fuel in (i)-(iii) & absorber in (iii)		absorber in (i)			absorber in (ii)	
	σ	σ_s	σ	σ_s		σ	σ_s
h	2.11228E-01	1.90001E-01 1.16636E-05	3.96908E-02	1.76684E-02	1.75847E-06	1.78882E-01	1.39293E-01 9.30325E-06
l	7.23458E-01	1.85926E-02 7.04384E-01	1.74551E-01	1.12667E-05	1.60722E-02	1.03217E+00	3.37989E-02 1.00381E+00

also fuel region: $(\sigma_{f,h}, \sigma_{f,l})$ = (3.01008E-04,1.01367E-02), (ν_h, ν_l) = (2.48225,2.43832), length: 5.5057cm, rod: 0.2794cm

Table 3: Data for the control rod problem; scatter cross sections are arranged as in (19).

As heterogeneity increases we get further away from the symmetric subproblem identified in section 3, so that we may expect a deterioration in the convergence rates. But note that even the homogeneous problem (iii) does not have full symmetry in its subproblem since the two energy groups introduce a non-symmetry due to the different scatter and fission rates for interactions from high to low, and low to high energies. In addition, we assumed vacuum boundary conditions for our analysis, while this model problem has reflective boundary conditions, so that our theoretical results are not directly applicable to this problem. But the numerical results are nevertheless interesting and give an indication for possible extensions of our analysis.

For our first test we used the same starting vector and stopping criterion as in the Los Alamos problem but changed the fixed shift to $\alpha_0 = 0.5$. With this and a constant inner tolerance $\tau_0 = 0.1$, we failed to converge to our demanded accuracy in all of cases (i)-(iii). Table 4 shows that the norm of the residual and the error in the eigenvalue do not decrease any further between 200 and 2000 iterations.

	$\tau_0 = 0.1$		$\tau_0 = 0.1$		$\tau_0 = 10^{-10}$		
	$\Delta^{(200)}$	$\|\widetilde{\mathtt{res}}^{(200)}\|_2$	$\Delta^{(2000)}$	$\|\widetilde{\mathtt{res}}^{(2000)}\|_2$	i	$\Delta^{(i)}$	$\|\widetilde{\mathtt{res}}^{(i)}\|_2$
pure absorber	8.17E-05	2.19E-06	8.17E-05	2.19E-06	5	4.00E-14	1.44E-15
absorber & water mix	3.14E-05	1.22E-06	3.14E-05	1.22E-06	6	2.00E-15	1.15E-15
homogeneous case	4.40E-06	3.32E-07	4.40E-06	3.32E-07	1	4.20E-14	3.77E-16

Table 4: Fixed shift $\alpha_0 = 0.5$; for $\tau_0 = 10^{-10}$ the problems converge within i iterations.

But the last column suggests that for a sufficiently small inner tolerance, convergence can be regained in practice. The statement that the homogeneous problem was solved after 1 iteration is no typing error but results from the fact that our starting vector of ones is almost an eigenvector in this case. So in order not to give problem (iii) an advantage for the remaining numerical tests, we changed our starting vector to one whose entries were chosen randomly in $(0, 1)$.

Table 5 gives numerical results for the cases (i)-(iii) using a fixed shift and decreasing tolerance. We obtain - as in the Los Alamos problem - linear but not quadratic convergence. In addition, we observe slightly faster rates for the more homogeneous problems (ii) and (iii) which could result from smaller jumps in the material cross sections and therefore an increase in the symmetry. But the more likely explanation is that the eigenvalues of problems (ii) and (iii) lie closer towards our chosen shift and the good convergence rates for all three cases suggest that the symmetry is not the driving force for convergence here.

	pure absorber			10% absorber, 90% water			homogeneous material		
i	$\Delta^{(i)}$	$\frac{\Delta^{(i)}}{\Delta^{(i-1)}}$	$\frac{\Delta^{(i)}}{(\Delta^{(i-1)})^2}$	$\Delta^{(i)}$	$\frac{\Delta^{(i)}}{\Delta^{(i-1)}}$	$\frac{\Delta^{(i)}}{(\Delta^{(i-1)})^2}$	$\Delta^{(i)}$	$\frac{\Delta^{(i)}}{\Delta^{(i-1)}}$	$\frac{\Delta^{(i)}}{(\Delta^{(i-1)})^2}$
1	2.16E-04			1.11E-05			5.40E-06		
2	7.89E-07	3.66E-03	1.70E+01	5.55E-08	4.99E-03	4.48E+02	1.21E-12	2.24E-07	4.16E-02
3	6.51E-09	8.25E-03	1.05E+04	3.30E-10	5.94E-03	1.07E+05	4.70E-14	3.87E-02	3.20E+10
4	5.57E-11	8.56E-03	1.32E+06	2.01E-12	6.10E-03	1.85E+07	3.60E-14	7.66E-01	1.63E+13
5	4.90E-13	8.80E-03	1.58E+08	2.11E-14	1.05E-02	5.22E+09	3.20E-14	8.89E-01	2.47E+13
6	6.02E-14	1.23E-01	2.51E+11						

Table 5: Control rod problem using a fixed shift $\alpha_0 = 0.5$ and $\tau^{(i)} \leq 0.1 \, \|P \, \widetilde{\mathbf{res}}\|_2$.

Our final table 6 illustrates the convergence properties using a constant tolerance and the non-standard Rayleigh quotient $\rho^{(i)}$ for the variable shifts $\alpha^{(i)}$. The results are poorer than in the Los Alamos problem suggesting something slightly better than linear but not quadratic convergence. This fits in well with our theory which made use of the underlying symmetry to guarantee quadratic convergence. As this problem is not symmetric we cannot expect quadratic convergence.

	pure absorber			10% absorber, 90% water			homogeneous material		
i	$\Delta^{(i)}$	$\frac{\Delta^{(i)}}{\Delta^{(i-1)}}$	$\frac{\Delta^{(i)}}{(\Delta^{(i-1)})^2}$	$\Delta^{(i)}$	$\frac{\Delta^{(i)}}{\Delta^{(i-1)}}$	$\frac{\Delta^{(i)}}{(\Delta^{(i-1)})^2}$	$\Delta^{(i)}$	$\frac{\Delta^{(i)}}{\Delta^{(i-1)}}$	$\frac{\Delta^{(i)}}{(\Delta^{(i-1)})^2}$
1	3.12E-05			2.60E-06			5.07E-06		
2	1.79E-07	5.72E-03	1.83E+02	3.56E-09	1.37E-03	5.24E+02	1.11E-08	2.19E-03	4.33E+02
3	4.43E-12	2.48E-05	1.39E+02	3.24E-12	9.11E-04	2.56E+05	4.45E-12	4.00E-04	3.59E+04
4	0.00E+00	0.00E+00	0.00E+00	3.00E-15	9.25E-04	2.85E+08	5.80E-14	1.30E-02	2.93E+09

Table 6: Results for the control rod problem with $\alpha^{(i)} = \rho^{(i)}$ and constant tolerance $\tau_0 = 0.1$.

Solving the same fixed tolerance problems with the standard Rayleigh quotient $\widetilde{\rho}^{(i)}$ gave similar convergence results to those in Table 6 without indicating superiority of one Rayleigh quotient over the other. Finally, using Rayleigh quotient shifts and decreasing tolerances, only 3 iterations were needed for convergence, making it difficult to establish the convergence rate. Looking at the total

number of iterations performed by GMRES (which is a good indicator for the work needed) for this problem and comparing it with the case of a fixed tolerance, shows a superiority of the decreasing tolerance for problem (ii) but similar amounts of work for the other two cases.

5 Conclusion

We provided a convergence analysis for inexact inverse iteration to solve the criticality problem in neutron transport theory for monoenergetic homogeneous model problems with isotropic scattering and vacuum boundary conditions. The theoretical results are supported by numerical experiments on a model problem with one space and one angular dimension, as well as by experiments on a more realistic physical problem which also has two energy levels and for which the theory offers useful practical guidance.

References

[1] E. J. Allen and R. M. Berry. The inverse power method for calculation of multiplication factors. *Annals of Nuclear Energy*, 20:922–950, 1983.

[2] M. Asadzadeh, L_p and eigenvalue error estimates for the discrete ordinates methods for two-dimensional neutron transport, *SIAM J. Numer. Anal.* 26:66-87, 1989.

[3] G. I. Bell and S. Glasstone. *Nuclear Reactor Theory*. Reinhold, 1970.

[4] J. Berns-Müller, I. G. Graham and A. Spence. Inexact inverse iteration for symmetric matrices. *Linear Algebra and its Applications*, 416:389–413, 2006.

[5] M. A. Freitag. Inner-outer Iterative Methods for Eigenvalue Problems - Convergence and Preconditioning. PhD Thesis, Department of Mathematical Sciences, University of Bath, 2007.

[6] M. A. Freitag and A. Spence. Rayleigh quotient iteration and simplified Jacobi-Davidson method with preconditioned iterative solves. *Linear Algebra and its Applications*, 428:2049–2060, 2008.

[7] H. Hochstadt. *Integral Equations*. Wiley-Interscience, 1973.

[8] C. Johnson and J. Pitkäranta. Convergence of a fully discrete scheme for two-dimensional neutron transport *SIAM Journal on Numerical Analysis*, 20:951-966, 1983

[9] L. V. Kantorovich and G. P. Akilov. *Functional Analysis*. Pergamon Press, 1982.

[10] E. E. Lewis and W. F. Miller, Jr. *Computational Methods of Neutron Transport*. John Wiley & Sons, New York, 1984.

[11] T. A. Manteuffel and K. J. Ressel. Least-squares finite-element solution of the neutron transport equation in diffusive regimes. *SIAM J. Numer. Anal.*, 35:806–835, 1998

[12] J. Mika. Existence and uniqueness of the solution to the critical problem in neutron transport theory. *Studia Mathematica*, 37:213–225, 1968.

[13] J. Pitkäranta and L. R. Scott. Error estimates for the combined spatial and angular approximations of the transport equation in slab geometry. *SIAM J. Numer. Anal.*, 20:922–950, 1983.

[14] B. P. Rynne and M. A. Youngson. *Linear Functional Analysis*. Springer Undergraduate Mathematics Series, Springer, London, 2008.

[15] A. Sood, R. A. Forster, and D. K. Parsons. Analytical benchmark test set for criticality code verification. Technical report, Los Alamos National Laboratory, 1999.

[16] W. M. Stacey. *Nuclear Reactor Physics*. Wiley, 2007.